Vol.67: e24220785, 2024
https://doi.org/10.1590/1678-4324-2024220785
ISSN 1678-4324 Online Edition

BABT
Brazilian Archives of Biology and Technology

Article - Engineering, Technology and Techniques

Biosorption of Sodium Dipyrone by Industrial Ash and Its Potential in Portland Cement Matrix

Luiza Lascosk[1*]
https://orcid.org/0000-0002-4585-5585

Eduardo Pereira[2]
https://orcid.org/0000-0001-6944-795X

Rodrigo Brackmann[3]
https://orcid.org/0000-0001-6948-0223

Juliana Martins Teixeira de Abreu Pietrobelli[1]
https://orcid.org/0000-0002-5804-1644

[1]Universidade Tecnológica Federal do Paraná (UTFPR), Departamento de Engenharia Química, Ponta Grossa, Paraná, Brasil; [2] Universidade Estadual de Ponta Grossa, Departamento de Engenharia Civil, Ponta Grossa, Paraná, Brasil. [3]Universidade Tecnológica Federal do Paraná (UTFPR), Departamento de Engenharia Química, Pato Branco, Paraná, Brasil.

Editor-in-Chief: Alexandre Rasi Aoki
Associate Editor: Alexandre Rasi Aoki

Received: 03-Oct-2022; Accepted: 12-Jan-2024

*Correspondence: luizalascosk@alunos.utfpr.edu.br; Tel.: +55-42-999177934 (L.L).

HIGHLIGHTS

- Biosorption process of sodium dipyrone with industrial ash was efficient.
- The ash after biosorption has the potential to be used as filler.
- Application of the circular economy concept, with the reuse of waste in biosorption and cement replacement in cement matrices.

Abstract: This research evaluated the use of industrial ash from eucalyptus chips in the biosorption of sodium dipyrone with the subsequent, study of its potential in Portland cement matrix. The biosorbent was characterized by the point of zero charge and the surface area. For comparison, before and after the biosorption process, scanning electron microscopy, energy dispersive x-ray spectroscopy, and Fourier transform infrared spectrometry were performed. Regarding the study of the potential of industrial ash after biosorption (AAB), it was characterized by analyzing specific mass, moisture, loss on fire, and X-ray fluorescence, as well as by X-ray diffraction, modified Chapelle, pozzolanic activity index with lime, and performance index with cement, compressive strength, and tensile strength by diametral compression. The biosorption tests were carried out in batch, it being possible to observe that at 298.15 K, 130 rpm, without pH adjustment approximately 93% of commercial dipyrone was removed. The pseudo-second-order kinetic model fitted better with the experimental data and the process was characterized as exothermic and spontaneous. The chemical composition of ash and AAB showed a predominance of CaO followed by MgO, without the presence of an amorphous halo. In the study of the filer effect, using cement pastes, both materials showed favorable results. Thus, it is concluded that the industrial ash studied has the potential to be applied as an alternative material in the removal of sodium dipyrone and for the replacement of cement in the composition of cement matrices, due to the filer effect they presented.

Keywords: biosorption; emerging pollutant; filler; mineral additions; Portland cement.

INTRODUCTION

It is necessary to pay special attention to contaminants of emerging problems, which must be constantly studied and must be monitored to minimize global damage. Sodium Dipyrone is one of the most used drugs in self-medication [1] and one of the most sold drugs in its different compositions and brands [2] so it is likely that after being metabolized, they reach the treatment stations and need alternative treatment.

Adsorption, an alternative process in the treatment of effluents, consists in the bonding of a liquid phase (solvent, usually water) containing a dissolved species, which is the adsorbate, to a solid phase referred to as an adsorbent. When the used material is composed of some type of biomass, we call it biosorbent and the process is called biosorption, an efficient and economical methods for the removal of contaminants with low concentrations [3-4].

In the biosorption process, the biosorbent application is measured by its effectiveness and feasibility of applying and it is related to characteristics such as the selectivity of the material; thermal and chemical stability; favorable kinetic and transport properties for rapid sorption; mechanical resistance; high capacity to be regenerated and low cost [5] and abundance.

The ash, residue from the burning of biomass in industrial boilers, has potential as a biosorbent, as it is generated in large quantities and its destination generates costs for industries. Currently, one of the options for the use of industrial ash is in agriculture as fertilizer, since has the action of correcting the soil due to its alkaline pH; another option is to use ash as compost [6-7]. Other ways of using ash occur in civil construction, as a viable alternative to reduce the amount of clinker in cement by the use of mineral additions, whether with filler effect, pozzolanic additions, or cementing agents [8]; and as adsorbents, being a low-cost and environmentally correct alternative for the treatment of industrial effluents [9], including the disposal of solid waste, such as ash.

The economic model of circular production proposes the regeneration of the value of capital and not just the extraction of this value, that is, it seeks a balance between the economy and the environment, combining the efficiency and effectiveness of the entire production system [10]. Circular Economy is based on three principles: 1. Preserve the value of natural capital, in order to control finite stocks and balance the flows of renewable resources, extending the useful life of the product; 2. Optimize resource production, resulting in limited, efficient and reduced use of primary resources, including waste collection, resource recycling, energy recovery and use of renewable energy; 3. Foster the efficiency of the system, minimizing negative externalities during the production and consumption cycle [11].

In this context, the present study aimed to evaluate the potential for removing the drug, sodium dipyrone, using the industrial residue, eucalyptus chip ash, as a biosorbent. As well as the determination of the potential of the material, after biosorption, for use as an addition in Portland cement matrices. This study combines the concept of Circular Economy to reinforce and boost its foundations in the socioeconomic environment.

MATERIAL AND METHODS

Preparation of solutions, calibration curve and sample reading

Aqueous solutions were prepared by the dissolution of Sodium Dipyrone (empirical formula $C_{13}H_{16}N_3NaO_4S.H_2O$.and molecular weight of 351.35 g mol^{-1}) in distilled water. The calibration curve was obtained from the standard solutions (0–100 mg L^{-1}), and the corresponding absorbance was obtained by the High-Performance Liquid Chromatograph – HPLC (YL Clarity 9100).

The reading of the samples was performed, after the centrifugation process, in the HPLC equipped with a pre-column, C-18 column (Phenomenex) and ultraviolet visible detector (UV-VIS), at 290 nm.

Biosorbent characterization

The biosorbent used in the tests (industrial ash) was provided by a Brewery in Ponta Grossa/PR. The biomass was dried at 303.15 K in an air-circulating oven with air renewal.

Point of zero charge test (pHpcz) was performed to evaluate the charge on the biosorbent surface. It was determined from samples containing 50 mL of sodium chloride (NaCl) solution (0.01 $mol.L^{-1}$), with the pH adjusted from 1 to 13 $\pm$ 0.1 and 0.15 g of biosorbent. After this, the final pH was determined, and data were plotted for pHpcz determination.

To determine the surface area of the biosorbent, pore volume and average pore diameter (B.E.T method) was employed a QUANTACHROME - Nova-1200 equipment with adsorption of N_2 at 77 K.

Scanning Electron Microscopy (SEM) was used to study the morphology of the material. The samples were prepared by depositing a thin layer of gold and palladium on their surface. Micrographs were obtained at a voltage of 20 kV and 100 times magnification using Tescan, Vega 3 LMU.

To analyze the surface's elemental composition of sample was used Energy-dispersive X-ray spectroscopy (EDS), also using Tescan, Vega 3 LMU.

The samples were analyzed by the Infrared Spectrophotometer (FTIR), model IRPrestige-21 with diffuse reflectance accessory, DRS-8000/Shimadzu. The analysis mode was % Transmittance, Number of Scans: 64, Resolution (cm^{-1}): 4, Minimum Interval (cm^{-1}): 400, Maximum Interval (cm^{-1}): 4000, by means of tablets pressed with KBr.

X-ray fluorescence (XRF) was used to chemical characterization, with the energy dispersive X-ray spectroscopy (EDX) method by the spectrometer model Rigaku ZSX Primus II.

X-ray diffractometry (XRD) was used to mineralogical characterization. The test was performed in a Rigaku Ultima IV diffractometer. The mineral chemical phases were identified through comparison with the ICDD (International Center for Diffraction Data) standards.

Experimental tests of biossorption

To determine the biosorption process, a set of tests was performed to determine the best-operating condition (temperature, agitation and pH) to be used in the subsequent tests: kinetic test, equilibrium and thermodynamic study. These tests were carried out with commercial samples of Dipyrone Sodium 1g (Novalgina 1g - SANOFI) using 50 mg. L^{-1} Dipyrone solutions.

Temperature effect test: this test was carried out at temperatures of 298.15, 308.15 and 318.15 K, lasting 6 hours and shaking at 130 rpm in a rotating shaking incubator (Tecnal, TE-240).

Agitation influence test: the test was performed at 65 and 130 rpm following the same methodology described in the analysis of the temperature effect test.

pH influence test: samples were prepared in 50 mL of dipyrone solution with a concentration of 50 mg L^{-1}. The pH adjustment was performed using concentrated solutions of HCl and NaOH in the ranges of 1 to 13. Subsequently, the samples followed the methodology of rotation, centrifugation and HPLC reading described above.

Kinect Test and Equilibrium Test

The kinetic test was performed to verify the time required to reach system equilibrium. This was carried out under the optimal conditions defined from the operational tests performed previously. Samples were analyzed at predetermined time intervals, between 0 and 1440 min (24h), which were centrifuged and read in HPLC. The kinetic parameters were obtained by fitting pseudo-first order, pseudo-second order, Elovich model and intraparticle diffusion kinetic models to the experimental data.

To evaluate the biosorption equilibrium, samples were prepared with concentrations between 10 and 500 mg L^{-1} at optimal pH, they were kept in the incubator with rotating agitation at 298.15 K, shaking at 130 rpm, for the equilibrium time that was obtained from the kinetic test.

Thermodynamic study

Enthalpy, entropy, and Gibbs free energy were studied from the results obtained in the kinetic study. The linear van't Hoff equation provides the relation for determining these parameters as a function of temperature, as expressed in equation (1).

$$\ln K_d = \frac{\Delta \mathrm{H}^\circ}{RT} + \frac{\Delta S^\circ}{R} \quad (1)$$

Where $\Delta \mathrm{H}^\circ$ is the enthalpy (kJ mol^{-1}); ΔS° the entropy (kJ mol^{-1} K^{-1}); R, the universal constant of ideal gases (8.314 J mol^{-1} K^{-1}); and T, the temperature (K).

Thus, $\Delta \mathrm{H}^\circ$ and ΔS° were determined by the graph of ln K_d versus 1/T, of the van't Hoff equation. Finally, the Gibbs free energy, $\Delta \mathrm{G}^\circ$ (kJ mol^{-1}), was calculated by equation (2).

$$\Delta \mathrm{G}^\circ = -\mathrm{R.T.} \ln K_d \quad (2)$$

The Arrhenius Equation was also used, which expresses the rate constant as a function of temperature and allows the determination of the activation energy, equation (3).

$$\ln(K) = \ln(k_A) - \frac{E_a}{RT} \quad (3)$$

Where $E_a =$ activation energy (J.mol^{-1}), $k_A =$ Arrhenius constant (g.mg-1.min^{-1}), $R =$ ideal gas constant (8,314 J.mol^{-1}. K^{-1}) and $T =$ temperature (K).

Potential in Portland Cement Matrix tests

The ash used in the biosorption tests was subsequently separated, by centrifugation, dried at 303.15 K in an oven with circulation and air renewal, for 3 hours, for later use in the characterization tests.

Ashes after biosorption (AAB) characterization

Specific mass: for the analysis of specific mass, the method adapted from NBR 16605 [12] was used.

Moisture: to determine the moisture (U), the methodology suggested by the Mercosur NM 24 standard [13] was used.

Modified Chapelle test: the modified Chapelle method aimeds to determine the pozzolanic activity of materials through the content of fixed calcium hydroxide by the method described in NBR 15895 [14].

The biosorbent, after biosorption, was characterized by Scanning Electron Microscopy (SEM), Energy-dispersive X-ray spectroscopy (EDS), Fourier transform infrared spectroscopy (FTIR), X-ray fluorescence (XRF) and X-ray diffractometry (XRD).

Pozzolanic tests

Pozzolanic performance index: the pozzolanic performance index of AAB with Portland cement at 28 days was determined according to NBR 5752 [15].

Index of pozzolanic activity with lime: the pozzolanic performance index with lime was determined according to NBR 5751 [16].

Study in cement paste with additions

For this study, cylindrical specimens of 20 x 50 mm Portland cement paste were molded, according to the mixing and molding procedure adapted from the NBR 7215 standard [17]. Four replacements (5%, 10%, 15% and 20%) of ash and AAB were studied.

Compressive strength: using 4 specimens for each percentage of replacement of ash and AAB, the compressive strength test was carried out, following the NBR 7215 [17].

Tensile strength by diametral compression: the tensile strength test by diametrical compression consisted of compressing the cylindrical specimens along the axial plane, with the aid of a press, defined by diametrically opposed generatrixes, coincident with the load application axis. The tensile strength by diametral compression was calculated by equation (4), according to the NBR 7222 [18].

$$f_{ct,sp} = \frac{2.F}{\pi.D.l} \quad (4)$$

Where $f_{ct,sp}$ is the tensile strength by diametral compression (MPa), F is the maximum force obtained in the test (N), D is the specimen diameter (mm) and l is the cylindrical specimen length (mm).

Water absorption by immersion and void ratio: the absorption and void index tests were adapted from the NBR 9778 standard [19].

The averages (before and after biosorption) were compared by the Tukey test at 5% level of significance ($p < 0.05$).

RESULTS

Biosorbent characterization

Point of zero charge test (pHpcz) is shown in Figure 1. The pHpcz found for industrial ash was approximately 10.00.

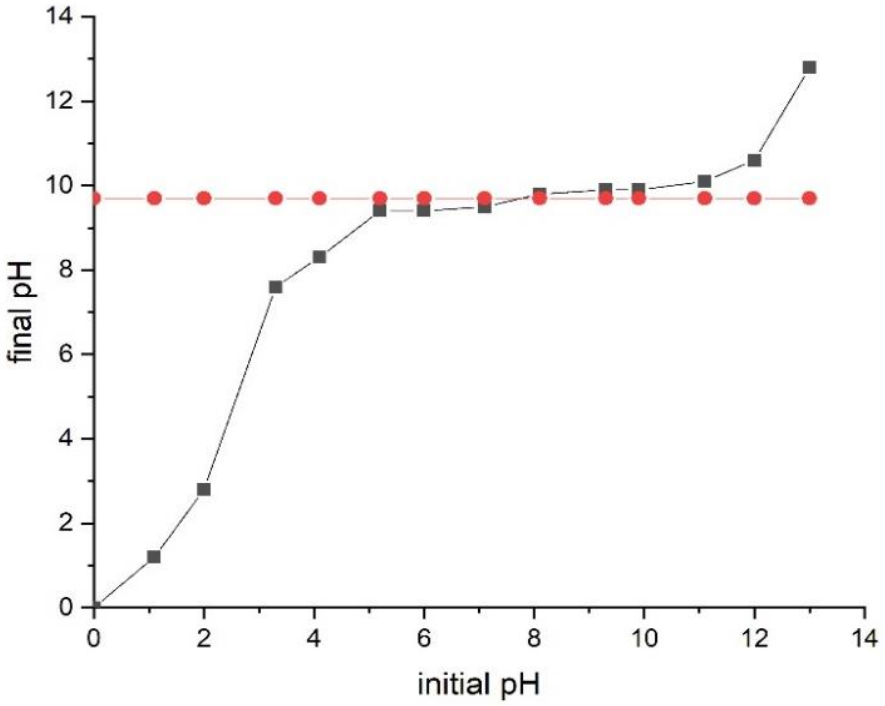

Figure 1. Point of zero charge test (pHpcz) of industrial ash.

Surface area of the biosorbent (S_{BET})*, pore volume* (p_V) *and average pore diameter* ($\bar{P}_D$)

Figure 2 shows the industrial ash adsorption/desorption isotherm.

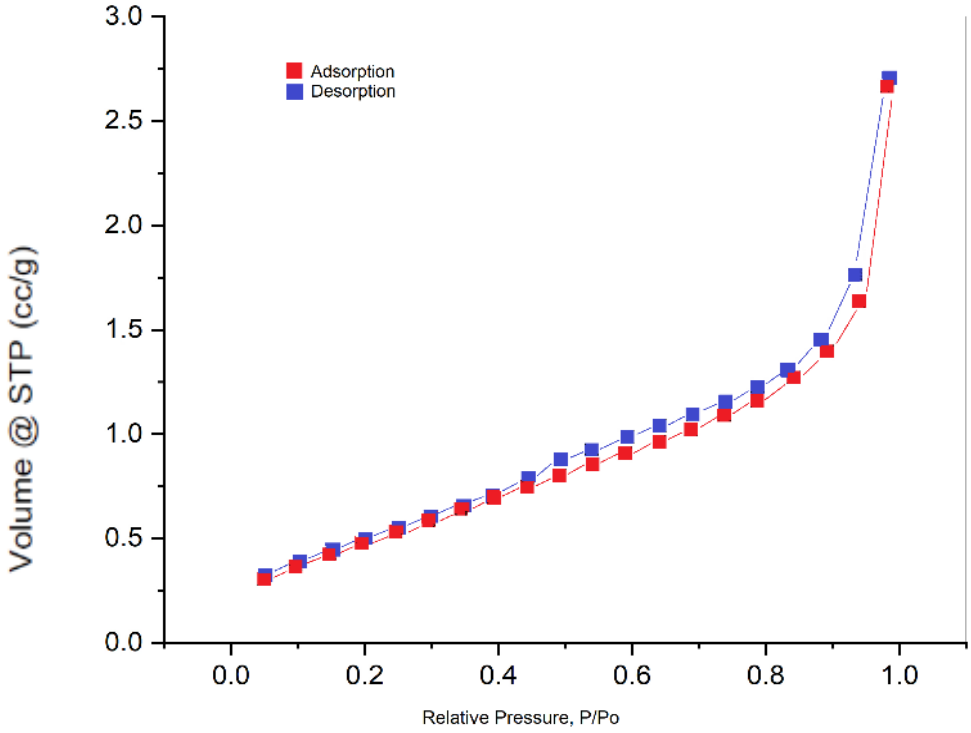

Figure 2. Adsorption and desorption isotherm of industrial ash.

The textural properties found for industrial ash by the BET method determined that the specific area (S_{BET}) was 1924 m^2/kg^{-1}, the pore volume (p_V) was 0.004195 cm^3/g^{-1} and the mean pore diameter ($\bar{P}_D$) was 4.361 nm.

Scanning electron microscopy: biomass micrographs before and after the dipyrone biosorption are shown in Figure 3(a) and (b), respectively.

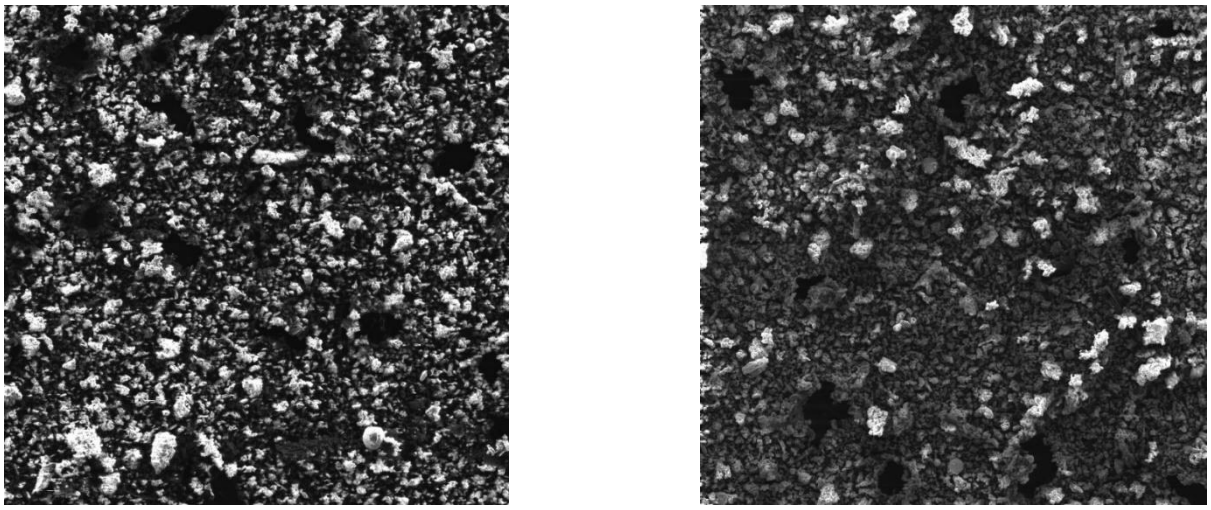

(a) **(b)**

Figure 3. SEM of the industrial ash (a) before and (b) after biosorption, 200x magnification.

SEM spectra shows in Figure 4 the representative bands of the elements in it. Analyzes were performed on ash before biosorption (a) and AAB (b).

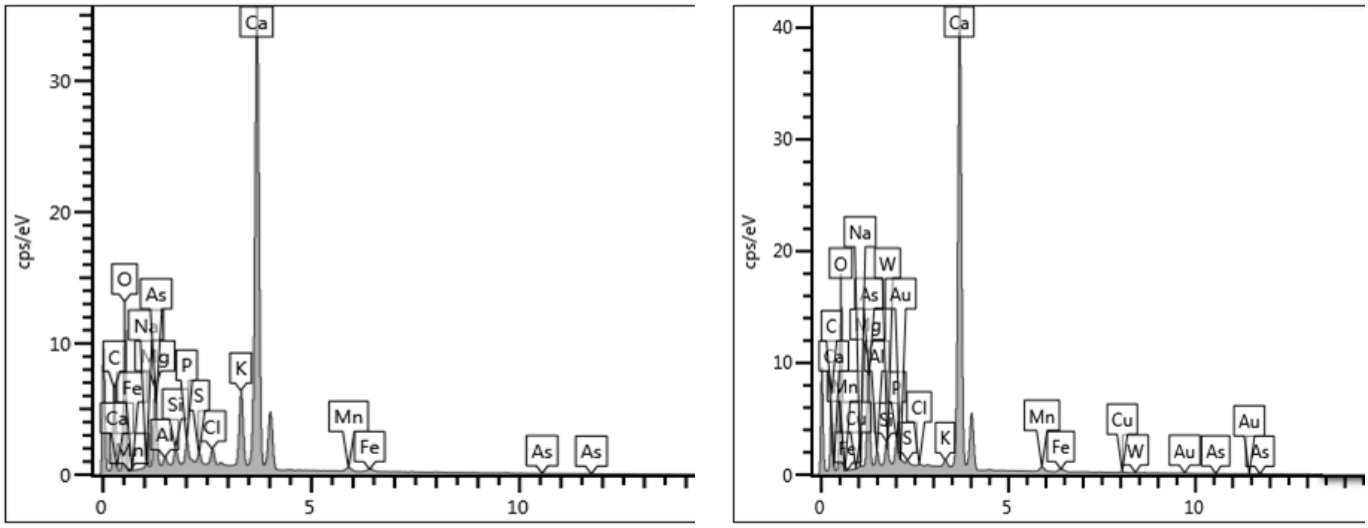

(a) **(b)**

Figure 4. SEM of the industrial ash (a) before and (b) after biosorption.

FTIR analysis: Infrared spectra of industrial ash, before and after biosorption, are shown in Figure 5.

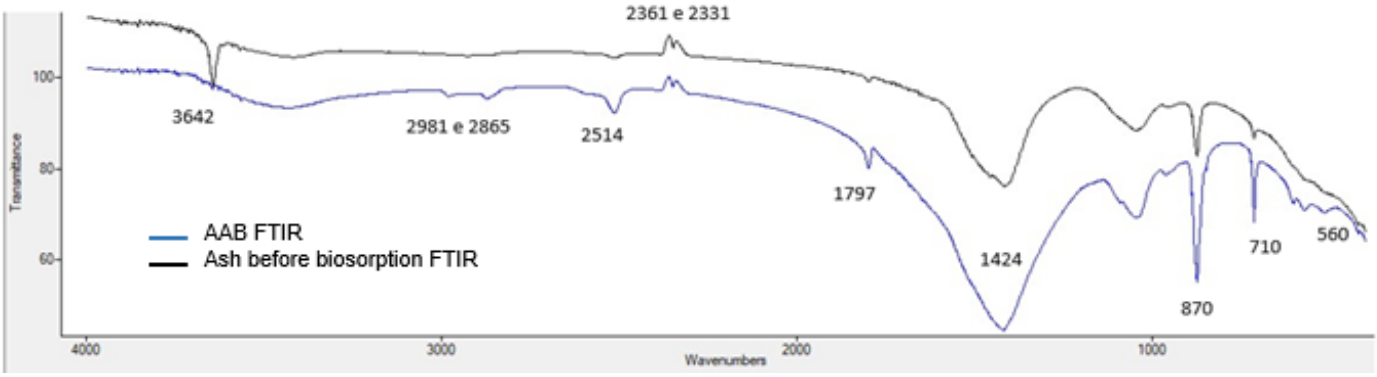

Figure 5. FTIR of the industrial ash before and after biosorption.

X-ray fluorescence (XRF): the chemical composition of industrial ash before and AAB, obtained by the XRF test, is shown in Table 1

Table 1. Chemical composition of the ash before and AAB.

	Chemical composition (%)													
Material	**Na_2O**	**MgO**	**Al_2O_3**	**SiO_2**	**P_2O_5**	**SO_3**	**Cl**	**K_2O**	**CaO**	**MnO**	**Fe_2O_3**	**SrO**	**ZnO**	**Total Alkalis**
Ash	0.244	9.95	0.964	2.20	3.45	0.520	0.508	5.99	73.60	1.22	1.08	0.278	-	4.1854
AAB	0.233	9.46	2.27	4.05	4.13	0.463	0.129	1.14	72.30	2.32	2.49	0.596	0.0672	0.9831

X-ray diffractometry (XRD): Figure 6 shows the X-ray diffractograms of industrial ash and AAB.

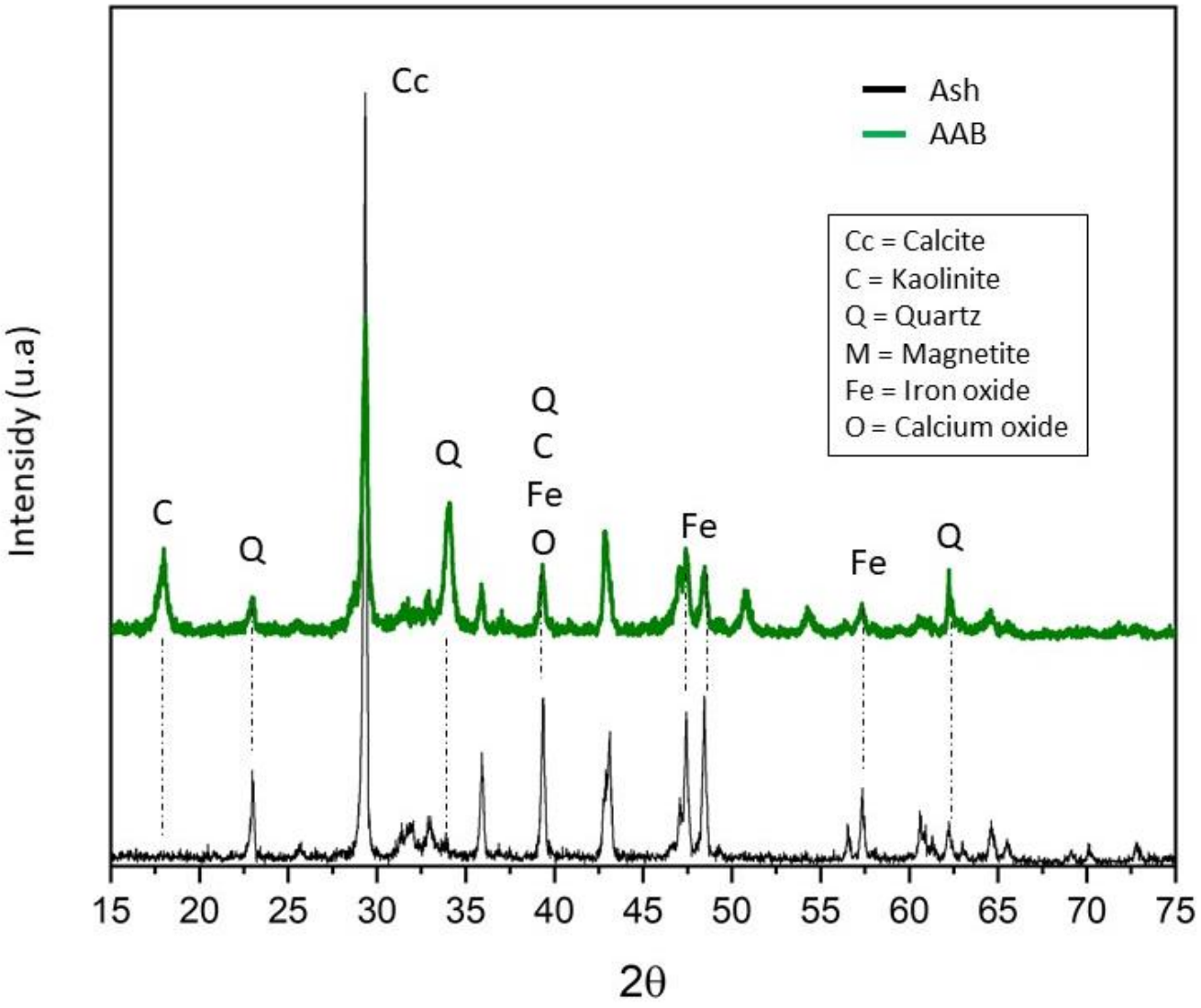

Figure 6. XRD of the industrial ash (a) before and (b) after biosorption

Experimental tests of biosorption

Temperature effect test and agitation influence test

Figure 7 (a) and (b) show the best removal conditions in terms of temperature and agitation, respectively.

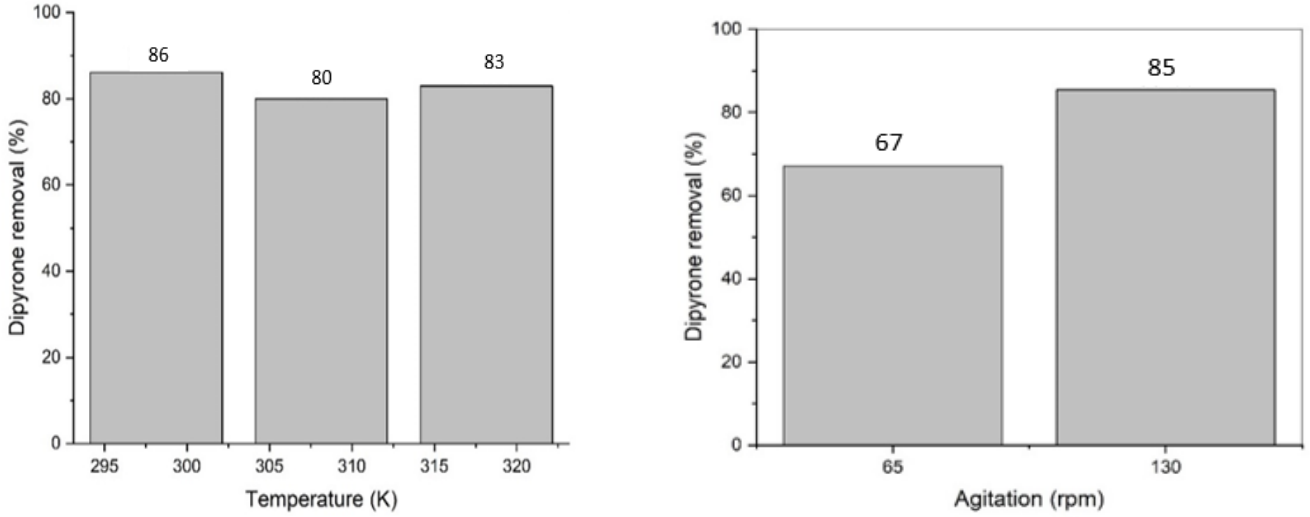

Figure 7. (a) Temperature effect test and **(b)** agitation influence test

pH influence test: Figure 8 shows the results in this test.

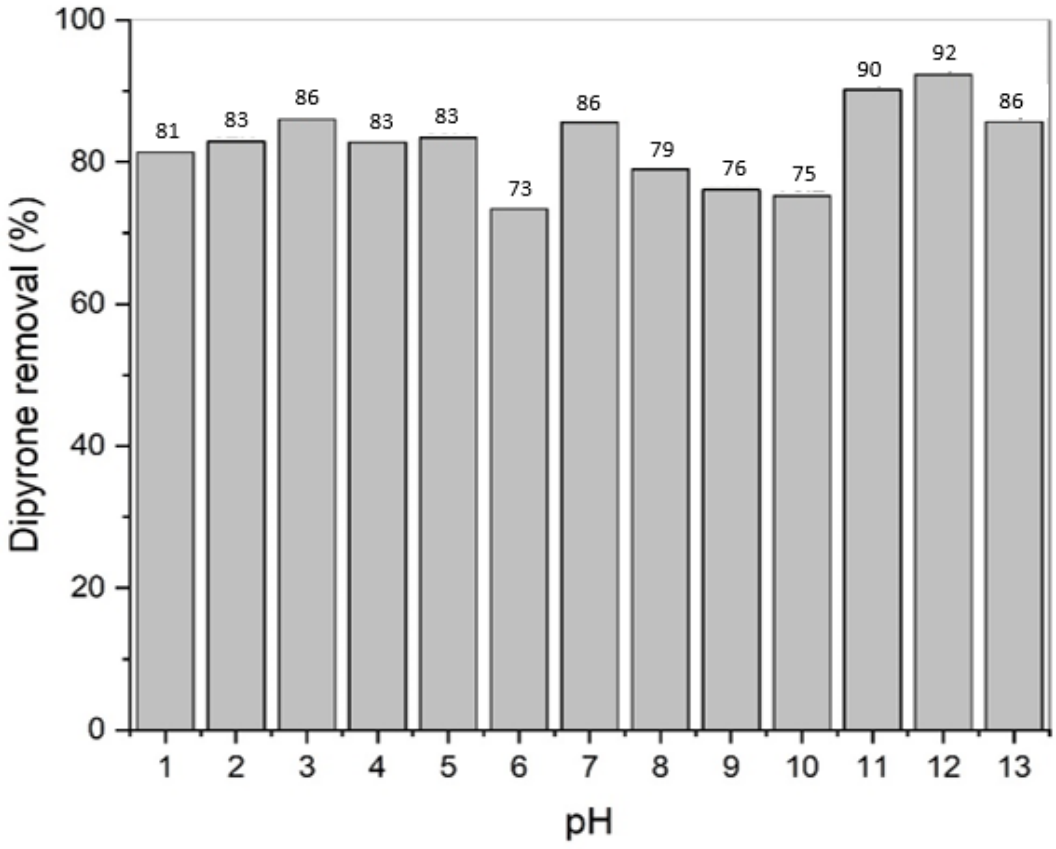

Figure 8. pH influence test.

Kinect Test

To start the kinetic study, the behavior of dipyrone removal by the ash was observed over time, at temperatures of 298.15, 308.15 and 318.15 K; then, kinetic models were used to evaluate the data. Figure 9 represents the observed behavior.

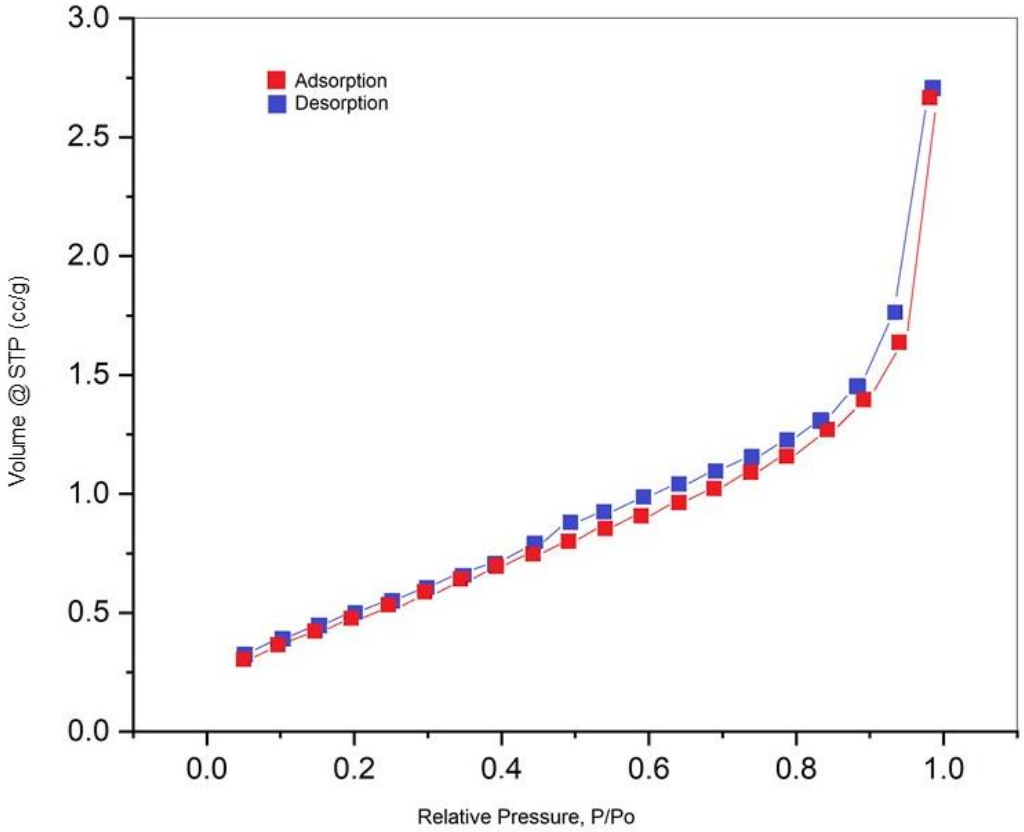

Figure 9. Effect of contact time on biosorption at different temperatures.

The adjustment of the kinetic models to the experimental data was performed from the mathematical software Origin 6.0 Demo and the parameters obtained by the models' adjustment are shown in Table 2.

Table 2. Kinetic parameters and determination coefficients of adjustment of kinetic models.

Models	**Parameters**
Pseudo-first order	$q_e = 4.713\ mg\ g^{-1};\ k_1 = 0.0967\ min^{-1}$ $R^2 = 0.7928$
Pseudo-second order	$q_e = 4.714\ mg\ g^{-1};\ k_2 = 0.3498\ min^{-1}$
Elovich	$R^2 = 1$ $\alpha = 4563.773\ mg\ g^{-1}min^{-1}$ $\beta = 3.1476\ mg\ g^{-1}min^{-1}$
Intraparticle diffusion	$q_e = 4.481\ mg\ g^{-1};\ R^2 = 0.7201$ $k_i = 0.0694\ mg\ g^{-1}min^{0,5};\ x = 3.164;\ R^2 = 0.2959$
Experimental data	$q_e = 4.820\ mg\ g^{-1}$ $equilibrium\ time = 360\ minutos$

Equilibrium Test

With the variation of the initial concentration of the sodium dipyrone solution, the biosorption equilibrium can be evaluated, since the equilibrium data of the amount of dipyrone in the solid phase (qe) and in the liquid phase (Ce) are related to generate the isotherm balance, according to the results presented in Figure 10.

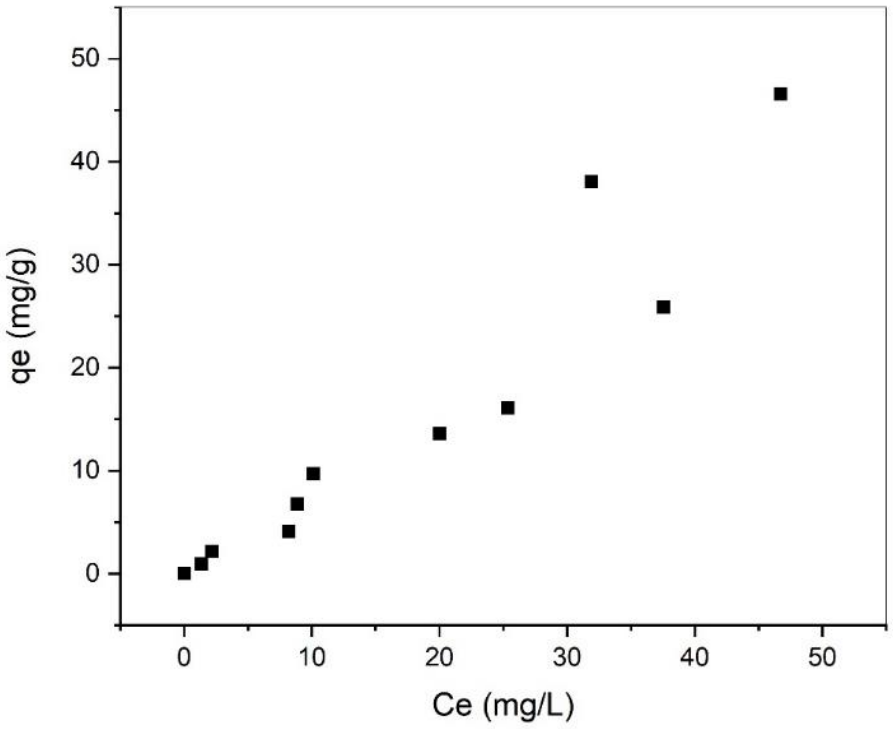

Figure 10. Experimental results of biosorption of Sodium Dipyrone by industrial ash.

Thermodynamic study

The parameters of activation energy, Gibbs free energy, enthalpy and entropy were obtained by applying equations 1 to 3. The equilibrium constants, k_d, were determined from the values of q_e and C_e obtained from Figure 10. The calculated parameters can be seen in Table 3.

Table 3. Thermodynamic parameters of biosorption of Sodium Dipyrone by industrial ash.

T (K)	k_d	$Ea\ (kJ/mol)$	$\Delta G°\ (kJ/mol)$	$\Delta H°\ (kJ/mol)$	$\Delta S°\ (J/K.mol)$
298.15	13.75		- 6.50		
303.15	10.75	24.017	- 5.99	- 71.61	59.07
318.15	7.30		- 5.26		

Ashes after biosorption (AAB) characterization

Specific mass, Moisture and modified Chapelle

Table 4 presents the results of density, moisture and modified Chapelle of the ash before biosorption and AAB.

Table 4. Specific mass, Moisture and modified Chapelle of industrial ash before and after biosorption.

Material	Specific mass (g/cm^3)	Moisture (%)	Modified Chapelle (mg $Ca(OH)_2$/g sample)
Ash	2.20	2.21	52.78
AAB	2.23	3.96	111.21

Pozzolanic tests

Pozzolanic performance index and *Index of pozzolanic activity with lime:*

Table 5 shows the results of Pozzolanic performance index and Index of pozzolanic activity with lime of industrial ash.

Table 5. Pozzolanic performance index and Index of pozzolanic activity with lime.

Parameter	% Substitution	Results
Pozzolanic performance index (MPa)	Reference	18.80
	Ash	17.41
Index of pozzolanic activity with lime (MPa)	Reference	18.80
	Ash	0.62

Study in cement paste with additions

Compressive strength, tensile strength by diametral compression, water absorption by immersion and *void ratio*

Table 6 presents the results of compressive strength, tensile strength by diametral compression, water absorption by immersion and void ratio.

Table 6. Compressive strength, tensile strength by diametral compression, water absorption by immersion and void ratio of industrial ash before and after biosorption.

Parameter	Ash		AAB	
	% Substitution	Results	% Substitution	Results
Compressive strength (MPa)	Reference	24.88	Reference	24.88
	5	21.38	5	21.13
	10	20.54	10	17.90
	15	21.06	15	19.43
	20	19.34	20	15.16
Tensile strength by diametral compression (MPa)	Reference	7.16	Reference	7.16
	5	5.02	5	2.01
	10	3.47	10	1.78
	15	5.09	15	1.45
	20	3.28	20	1.64
Water absorption by immersion (%)	Reference	16.30	Reference	16.30
	5	19.30	5	17.80
	10	21.70	10	20.10
	15	17.60	15	20.30
	20	19.60	20	21.70
Void ratio (%)	Reference	14.00	Reference	14.01
	5	16.10	5	15.10
	10	17.70	10	16.70
	15	14.90	15	16.80
	20	16.30	20	17.80

DISCUSSION

From the experimental data (Figure 1), it is observed that the PCZ found for industrial ash was approximately 10.00. With the pH tests, a pH of 7.30 was obtained for the sodium dipyrone solution and a pH of 11.96 for the sodium dipyrone solution with industrial ash. With these data, the pH > PCZ, which indicates that the solid adsorbent is negatively charged in the solution, as the pH is higher than the PCZ, and that it may interact with positive metallic species [20].

The results obtained studying surface area of the biosorbent (S_{BET}), pore volume (p_V) and average pore diameter ($\bar{P}_D$) agree with the ranges found in comparison with the referenced works, considering the variability that the ashes have. The material studied can be classified as mesoporous ($\bar{P}_D$) between 2 nm and 50 nm) [21], which is in accordance with the isotherm obtained in Figure 2, which can be classified as a Type 5 Isotherm, characteristic of this material classification.

At Scanning electron microscopy, it is possible to observe the irregular shape of the particles, as well as a great surface roughness. Such characteristics were also observed in wood ash micrographs [22]. A greater presence of pores is observed in Figure 3 (a) when compared to Figure 3 (b), such occurrence can be justified by the fact of the effective biosorption of sodium dipyrone by the ash, which corroborates the definition of good biosorbent materials.

Analyzes were performed in *SEM* spectra (Figure 4), on ash before biosorption (a) and AAB (b). It is possible to observe the predominance of the elements Calcium (Ca), Oxygen (O_2), Carbon (C), Magnesium (Mg) and Potassium (K) in the ash before the biosorption and in the AAB it is also observed the predominance of the element Calcium (Ca), followed by the presence of Oxygen (O_2), Carbon (C) and Magnesium (Mg).

The results of FTIR spectra of industrial ash, before and after biosorption shows the functional groups that stand out are the stretching of OH^- at 3642 cm^{-1}, the vibrations related to $^-CH3$ at 2981 cm^{-1} and to $^-CH_2$ at 2865 cm^{-1}, the stretching at 1797 cm^{-1} which is due to the C=O bond, the presence of calcium carbonate (calcite) at 870 cm^{-1}, 1424 cm^{-1} and 2514 cm-1 [23-24] and the stretching at 710 cm^{-1}, resulting from a deformation in the plane (O-Si-O).

It is observed that the compound with the highest percentage is Calcium Oxide, followed by Magnesium Oxide in X-ray fluorescence (XRF) analysis, such compounds were identified in previous analysis.

X-ray diffractometry (XRD) was carried out to determine whether the additions have an amorphous halo in their diffractograms, which is characteristic of pozzolans, given that the reactivity of the addition is related to the amount of material that is in the amorphous state [25]. Analyzing the diffractogram peaks, it is observed that the main crystalline phase existing in the in industrial ash and in the AAB is calcium carbonate, confirming the results obtained in the XRF and SEM analyses; there are also amounts of quartz, kaolinite ($Al_2Si_2O_5(OH)_4$), magnetite (Fe_3O_4), iron oxide (Fe_2O_3) and calcium oxide (CaO). CAB also did not present amorphous halo, so, considering this test, it is not possible to attribute pozzolanic potential to the material. Small variations are observed in the structures found when comparing the materials studied, that is, the mineralogy is basically the same. When the crystalline structures are well defined and stable, it can be said that there is no pozzolanic activity in the materials [26].

For the experimental tests of biosorption at the temperatures analyzed (298.15, 308.15, and 318.15 K) it was observed that the best removal of dipyrone occurred with the process at 25ºC and obtained a value of 86.05% removal (Figure 7 (a)). It is observed that for all evaluated temperatures, the behavior was similar. The study to evaluate the influence of agitation was carried out by evaluating the percentage of dipyrone removal at values of 65 rpm and 130 rpm (Figure 7 (b)). From the result obtained, it can be noted that the agitation of 130 rpm promotes a higher percentage of removal in the process, a fact that can be associated with the greater surface contact area achieved during the agitation of the solutions. The pH influence test *(*Figure 8) observed that the best removal percentages are in the range from pH 11 to pH 13, with the highest removal being found at pH 12 (92.55%). Based on these results, and to avoid changes in the solution regarding its pH, the use of dipyrone solution without pH change was adopted.

In the kinetic study, a rapid removal of dipyrone by the ash was obtained in the initial minutes, where in approximately 10 minutes there was already a removal of around 85%. It is also noted that this rate became slower until reaching equilibrium (360 minutes) and removal of 93.23% was obtained. Other dipyrone removal systems obtained removal of 70% (removal with activated carbon) [27], 80% (heterogeneous catalysis using TiO2/UV) [28] and 50.36% (UV-vis with pH variation) [29]. Thus, it is noted that the efficiency achieved in this work is significant.

The adjustment of the kinetic models to the experimental data and the parameters obtained show that the model that best fitted the data obtained was the pseudo-second order model, with correlation coefficient $R^2 = 1$. In this model, it is known that the limiting step of the biosorption process is chemisorption and that there is the involvement of forces of sharing or exchange of electrons between the sorbate and the sorbent [30].

At the equilibrium test, the behavior of a linear isotherm is observed. The linear isotherm is observed under conditions in which the number of active sites remains constant over the entire range of solute concentrations until substrate saturation. This means that the surface available for adsorption expands proportionally with the amount of solute adsorbed [31].

And about the thermodynamic study, the activation energy value obtained was 24.017 kJ mol^{-1}, which classifies the biosorption process as physisorption (Ea value between 5 to 40 kJ mol^{-1}).

The increase in $\Delta G°$ values with increasing temperature indicates that adsorption is more favorable at lower temperatures. In addition, negative values of Gibbs free energy indicate that the process occurs spontaneously, so the more negative $\Delta G°$ is, the easier the contaminant removal process is [32].

The negative value related to the enthalpy variation ($\Delta H° = -71.61$ kJ mol^{-1}) reveals that the interaction between the active sites of the ash particles with sodium dipyrone is exothermic in nature. As the value obtained is less than 40 kJ mol^{-1}, the process presents physisorption characteristics, which possibly occur through Van der Waals bonds [34]. This fact indicates that the lower the temperature, the greater the biosorption efficiency, a fact confirmed by the temperature influence test and kinetic test.

And about entropy, the positive value found for entropy ($\Delta S° = 59.07$ J K^{-1} mol^{-1}) indicates an increase in entropy due to adsorption, meaning an increase in randomness at the solid/solution interface, due to changes in the adsorbate and in the adsorbent, and the affinity of the adsorbent for the adsorbate [34].

In the tests that characterized the AAB after the biosorption process, the value of the specific mass of the ash before and AAB were close to each other, 2.20 g cm^{-3} and 2.23 g cm^{-3}, respectively. Some studies found specific mass values for eucalyptus chip ash between 1.12 g cm^{-3} [35] to 2.81 g cm^{-3} [36].

The values for the moisture of industrial ash are within the requirement required by NBR 12653 [37] which guides that the moisture of pozzolanic materials must be less than or equal to 3%; the AAB exceeded the value required by the standard and can be classified as a filler.

To be considered a pozzolanic material, from the point of view of the Modified Chapelle test, it is necessary that the material present 330 mg CaO/g pozzolan, which corresponds by stoichiometry to 436 mg $Ca(OH)_2$/g pozzolan [38]. It is observed that both ashes do not meet the requirement to be considered pozzolanic material, because in their composition there is no amorphous silica and aluminum available to react in a pozzolanic way.

At pozzolanic test, the average presented by the reference was 17.14 MPa and the material obtained a satisfactory result. But for the material to be considered pozzolanic, it must have a compressive strength ≥ 6 MPa [39]. It can be seen from the result obtained that the industrial ash had a result below the minimum limit designated by the referred standard.

At the study in cement paste with additions, the percentage of replacement that showed the best result was in the replacement of 5% and 15% for the ashes and the AAB, since there is no statistical difference between the values obtained. Although the percentage of replacement exceeds the value that the regulations suggest for replacement (25%) [39], with the data obtained, it was found that a total replacement of 30% is also possible, since it did not compromise the strength of the materials.

The results obtained suggest, as well as for the water absorption by immersion and for the void index, that the studied substitutions resulted in relatively higher values compared to the specimens without addition due to the specific mass of the materials; with this, it can be concluded that cement matrices with higher ash contents tend to be more porous, which justifies the higher absorption values.

The ash, which can be used as filler, is an economically viable solution [40], as it the disposal of ash in civil construction is considered cheap and environmentally clean [41].

CONCLUSION

The industrial ash studied proved to be efficient in the biosorption process of Dipyrone Sodium in aqueous solution, the process performed better at 25 ºC, 130 rpm, without pH adjustment, for 360 minutes, with 93.23% of commercial dipyrone removed. It is emphasized that the ambient temperature and the absence of the need to adjust the pH, makes the industrial application more favorable and the process friendlier, since there is no addition of reagents to adjust the pH and neither the energy expenditure to increase the temperature.

The ash and the AAB had a satisfactory performance in the study of the filer effect, through substitutions in cement pastes. Thus, their respective uses are promising in the partial replacement of cement in the composition of cement matrices, with the replacement of 10% or 15% being the replacements with the best performance in the properties analyzed.

The circular economy is based on the reuse of waste, in which wastes are inputs to produce new products. In this work, it was found that the ash studied was successful in the biosorption process, removing the sodium dipyrone present in aqueous solution and, also, that the ash can be used as a filler in the cementitious replacement in cement matrices. It is observed the valorization of this residue, since it was used in the treatment of liquid effluent and, later, used as an input in the production of a new product, with cementitious characteristics.

Funding: This research received no external funding.
Acknowledgments: The authors thank the technical support from the Multiuser Characterization Center in Materials Research and Development (C2MMa) and the Laboratory of Destructive and Non-Destructive Tests located (LabENS) at the Universidade Tecnológica Federal do Paraná, Campus Ponta Grossa, as the Multiuser Laboratory for Research Support (Lamap) at Universidade Tecnológica Federal do Paraná, Campus Apucarana. As well as the C-LABMU - Multiuser Complex of Ponta Grossa State University.
Conflicts of Interest: The authors declare no conflict of interest.

REFERENCES

1. Arrais PSD, Fernandes ME, Da Silva DPT, Ramos LR, Mengue SS, Luiza VL, et al. Prevalence of self-medication in Brazil and associated factors. Public Health Magazine, [s.I.]. 2016 v. 50(3).
2. Interfarma, GUIDE 2019. Nebraska Composição Gráfica. Brasil, 2019.
3. Lenzi GG, Fuziki MEK, Fidelis MZ, Fávaro YB, Ribeiro Map, Chaves ES, et al. Caffeine Adsorption onto Bentonite Clay in Suspension and Immobilized. Braz Arch Biol Technol. 2020 Vol.63.
4. Da Silva BC, Zanutto A, Pietrobelli JMTA. Biosorption of reactive yellow dye by malt bagasse. Adsorpt Sci Technol JCR, 2019; 1(2).
5. Seader, JD, Henley, EJ, Roper, DK. Separation Process Principles: Chemical and Biochemical Operations. 3. ed. Hoboken, NJ: Wiley, c2011. John Willey & Sons, Inc. 2010, 822.
6. Da Costa, TP. Environmental assessment of valorization alternatives for woody biomass ash in construction materials. Resour, Conserv Recycl. 2019, 148: 67-79.
7. Milovanović B, Stirmer N, Cerevic I, Bericevic, A. Wood biomass ash as a raw material in concrete industry. Građevinar. 2019, 71(6): 505-14.
8. Brekailo F, Pereira E, Pereira E, Farias MM, Medeiras-Junior RA. Red ceramic and concrete waste as replacement of Portland cement: Microstructure aspect of eco-mortar in external sulfate attack. Cleaner Materials 2022, 3 (100034).
9. Cacuro TA, Waldman WR. Ash from biomass burning: applications and potential. Virtual Chemistry Magazine. 2015; 7 (6): 2154-65.
10. Gonçalves TM, Barroso AF da F. The circular economy as an alternative to the linear economy. Proceedings of the XI Sergipe Production Engineering Symposium. 2019; Sergipe, Brazil. ISSN 2447-0635.
11. Ellen Mac Arthur Foundation. Circular Economy. 2017. Avaible from: https://www.ellenmacarthurfoundation.org/pt/economia-circular-1/principios-1.
12. ABNT – Brazilian Association of Technical Standards. NBR 16605: Portland cement and other powdered materials – Determination of specific gravity. 2017. Brazil (4).
13. ABNT - Brazilian Association of Technical Standards. NBR 24:2002: Pozzolanic materials – Determination of moisture content Brazil. 2002 (2).
14. ABNT - Brazilian Association of Technical Standards. NBR 15895: Pozzolanic materials – Determination of fixed calcium hydroxide content – Modified Chapelle Method. Brazil. 2010 (6).
15. ABNT - Brazilian Association of Technical Standards. NBR 5752: Pozzolanic materials – Determination of the performance index with Portland cement at 28 days. Brazil. 2014 (4).
16. ABNT - Brazilian Association of Technical Standards. NBR 5751: Pozzolanic materials – Determination Of pozzolanic activity with lime after 7 days. Brazil. 2012 (4).
17. ABNT - Brazilian Association of Technical Standards. NBR 7215: Portland Cement – Determination of compressive strength. Brazil, 2014 (8).
18. ABNT - Brazilian Association of Technical Standards. NBR 7222:Concrete and mortar – Determination of tensile strength by diametrical compression of cylindrical specimens. Brazil. 2010 (7).
19. ABNT - Brazilian Association of Technical Standards. NBR 9778: Cemente and mortar – Determination of water absorption, void index and specifi mass. Brazil. 2005 (4).
20. Silva, MVR. Adsorption of hexavalent chromium by comercial granulated activated carbono in the presence of anionic surfactante (LAS) [dissertation]. Brazil: Federal University of Pará; 2012. 80p.
21. IUPAC. International Union of Pure and Applied Chemistry, 2013. Avaible from: http://www.iupac.org/home/about.html.
22. Ban CC, Ramli M. The Implementation of Wood Waste Ash as a Partial Cement Replacement Material in the Production of Structural Grade Concrete and Mortar: An Overview. Resources, Conservation and Recycling. 2011. 55: 669-85.
23. Learner T. The use of a diamond cell for the FTIR characterization of paints and varnishes available to twentieth century artists. IRUG2 Meeting. 1995 (7-25). Avaible from: http://www.irug.org/documents/1Learner.pdf.
24. Bessler, KE, Rodrigues, LC. Calcium carbonate polymorphs – and easy synthesis of aragonite. Scielo. 2007 Dez; 31(1). Avaible from: http://www.scielo.br/scielo.php?script=sci_arttext&pid=S0100- 40422008000100032.
25. Gobbi, A. Pozzolanic activity of mineral additions by NBR 5751/2012 and NBR 5752/2012: a critical analysis based on complementary methods [dissertation]. Brazil: Federal University of Paraná; 2014.110p.
26. MOURA, LS. Characteritzaion of the pozzolanic activity of mesquite ash produced at different temperatures. 20º Brazilian Congresso of Engineering and Materials Sciences (CBECiMat). Joinville. Brazil; 2012.
27. Santos, KRA, Santos, LS, Rodrigues, CC, Da Nóbrega, SW. Competitive adsorption of drugs in aqueos matrix. Congress ABES FENASAN. Brazil; 2017.
28. Terra, SDV, Goulart, BV, Fagundes, PMLL, Nadaleti, DHS, Kondo, MM. Photodegradation of dipyrone by heterogeneous catalysis using TiO2/UV. Res. Soc. Devt. 2020; 9(1).
29. Isquibola, G, Rodrigues, EC. Degradation study of commercial sodic dipyrone through the ultraviolet light and visible light. Brazilian Journal of Scientific Initiation (RBIC). 2019; 6 (7): 82-93.
30. Ho YS, Mckay G. Pseudo-second order model for sorption processes. Process Biochem. 1999; 34:451–65.
31. Giles, CH, Smith, D, Huitson, AA. General Treatment and Classification of the Solute Adsorption Isotherm I. Theoretical. J Colloid Interface Sci. 1974,47(3).

32. Zhang, ZG, Mao, Z, Liu, X, Zhang, YG, Brodholt, J. Stability and Reactions of CaCO3 Polymorphs in the Earth's Deep Mantle. J Geophys Res. Solid Earth. 2018, 123: 6491-500.
33. Al-Degs Y, Khraisheh MAM, Allen SJ, Ahmad MN. Effect of carbon surface chemistry on the removal of reactive dyes from textile effluent. Water Res. 2000, 34 (3): 927-35.
34. Mohan, D, Singh, KP, Singh, G, Kundan, K. Removal of Dyes from Wastewater Using Fly ash, a Low-Cost Adsorbent. Ind. Eng. Chem. Res. 2002, 41: 3688-95.
35. Resende, DS. Bezerra, ACS, Gouveia, AC, Aguilar, MTP. Radispiel Filho, H, Keles, JG. Eucalyptus Chip Ashes in Cementitious Composites. Mater Sci Forum JCR, 2014. 775-776: 205-9.
36. Couto, AF, Scwantes-Cezario, N, Morales, G, Toralles, BM. Preliminary evaluation of the effects os partial replacement of fine aggregate with Eucalyptus Wood Ash (CME) on mortar properties. Civ Eng J (IMED). 2018, 5 (2).
37. ABNT - Brazilian Association of Technical Standards. NBR 12653: Pozzolanic materials - requeriments. Brazil, 2014 (10).
38. Raverdy M, Brivot, F, Paillere, AM, Dron, R. [Evaluation of the pozzolanic activity of secondary constituents]. In: 7th Int. Congr. Chem. Cem. Paris, 1980.
39. ABNT - Brazilian Association of Technical Standards. NBR 16697: Portland Cement - requeriments. Brazil, 2018.
40. Zanoletti A, Ciacci L. The Reuse of Municipal Solid Waste Fly Ash as Flame Retardant Filler: A Preliminary Study. Sustainability. 2022,14:2038.
41. Bakalar T, Pavolova H, Hajduova Z, Lacko R, Kysela K. Metal recovery from municipal solid waste incineration fly ash as a tool of circular economy. J Clean Prod. 2021, 302.